Three simulations of Optical Communication System Course(EE244) Project

Jinze Shi, *Shanghaitech University*

***Abstract*—This thesis reported three simulations' background and results of course project of optical communication system (EE244, Shanghaitech University) based on software Optisystem. Including DFB laser parameter sweep, muti-mode fiber mode coupling and gain's effect on QAM modulation.**

***Index Terms*—Optisystem, DFB laser, Muti-mode Fiber, QAM Modulation**

I. DFB LASER SIMULATION

A. Introduction of FP, DFB and DBR laser

Fabry-Perot (F-P) Laser, Distributed Feedback (DFB) Laser, and Distributed Bragg Reflector (DBR) Laser are different types of semiconductor lasers that are widely used in various applications, such as telecommunications, sensing, and spectroscopy. They differ in their construction, working principles, and performance characteristics. Here, working principles of these three types of lasers and a comparison among them were analyzed.

The Fabry-Perot laser consists of a gain medium sandwiched between two parallel mirrors. When an electrical current is applied to the gain medium, it emits light, which is reflected back and forth between the mirrors. This process causes the light to amplify and leads to lasing action. The laser output is emitted through one of the mirrors, which is partially reflective. It has simpler structure and it's manufacture is easier, leading to lower costs and high output power. The drawbacks are less precise control over the lasing wavelength, resulting in multiple longitudinal modes and a broader spectral output and higher sensitivity to temperature changes, affecting the lasing wavelength.

A DFB laser has a periodic grating structure incorporated within the gain medium, which serves as a wavelength-selective element. The grating provides feedback only at a specific wavelength, ensuring single longitudinal mode operation. This results in a narrow linewidth and stable wavelength output. The advantages of DFB laser are single longitudinal mode operation, leading to a narrow linewidth and high spectral purity and more stable operation, with lower sensitivity to temperature changes compared to F-P lasers. While it has more complex manufacturing process due to the requirement of a periodic grating and lower output power compared to F-P lasers.

The Bragg Wavelength of DFB laser is ralated with the grating of periodicity:

$$\lambda_B = 2n_{eff}\Lambda \tag{1}$$

The wavelength of the laser is represented by:

$$\lambda = \lambda_B \pm \frac{\lambda_B^2}{2n_e L_e}(m + 1/2) \tag{2}$$

for m = 0:

$$\Delta\lambda = \frac{\lambda_B^2}{2n_{eff}L_e} \tag{3}$$

$$\lambda_B = \frac{\lambda_2 - \lambda_1}{2} \tag{4}$$

For example two modes with 1549nm and 1551nm:

$$\lambda_B = 1550nm \tag{5}$$

DBR laser is similar to a Fabry-Perot laser but has Bragg reflectors at one or both ends instead of simple mirrors. These Bragg reflectors are made from alternating layers of materials with different refractive indices, which selectively reflect specific wavelengths. This allows for better control over the lasing wavelength and spectral purity. It has better control over the lasing wavelength and spectral purity and less sensitive to temperature changes compared to F-P lasers. But it's drawbacks are more complex manufacturing process due to the need for Bragg reflectors, lower output power and more expensive to manufacture.

In sum, Fabry-Perot lasers have simpler structures, making them easier and cheaper to manufacture. However, they exhibit broader spectral outputs and are more sensitive to temperature changes. DFB and DBR lasers provide better control over the lasing wavelength and improved spectral purity, making them suitable for applications requiring precise wavelength control. However, they have more complex manufacturing processes and can be more expensive to produce.

B. Simulation of L-I curve and Front Facet Reflectivity Optimization

From Figure.2, the threshold current for parameters 1 is about 22.8475mA.

From Figure.3, the threshold current for parameters 1 is about 18.2624mA.

From Figure.4, the maximum output power corresponding front facet reflectivity is about 0.00964816. (Sweep range is finally restricted to log scale 0.001 to 0.015 after many times sweep)

From Figure.5, the gap is about 2.1499nm, and the Bragg Wavelength is about 1.549985nm.

In summary, the facet reflectivity affects the stability, output power, and efficiency of a DFB laser by influencing unwanted

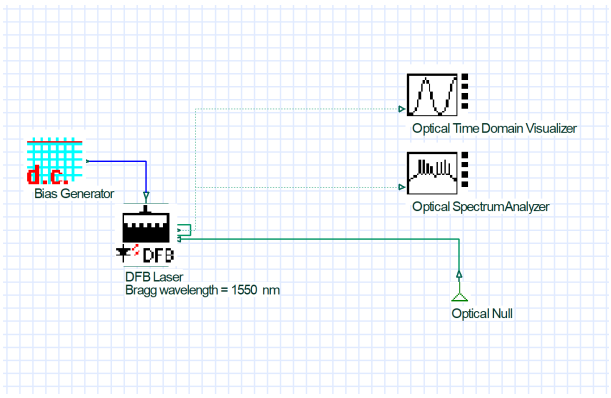

Fig. 1. Simulation Set up

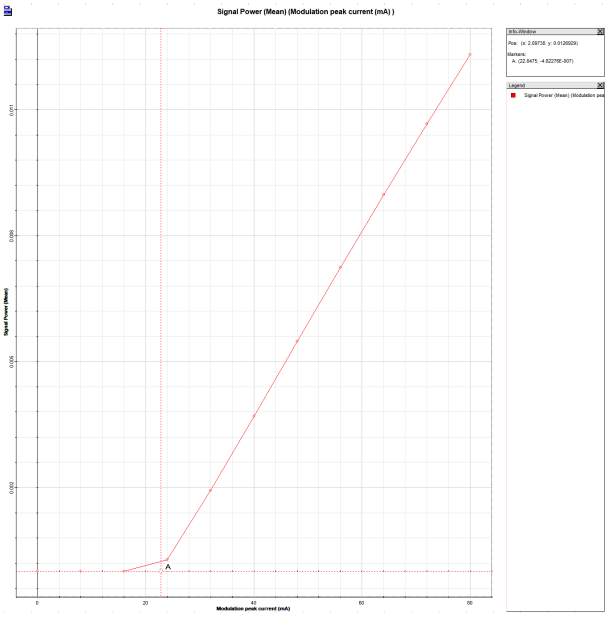

Fig. 2. L-I curve of parameters 1

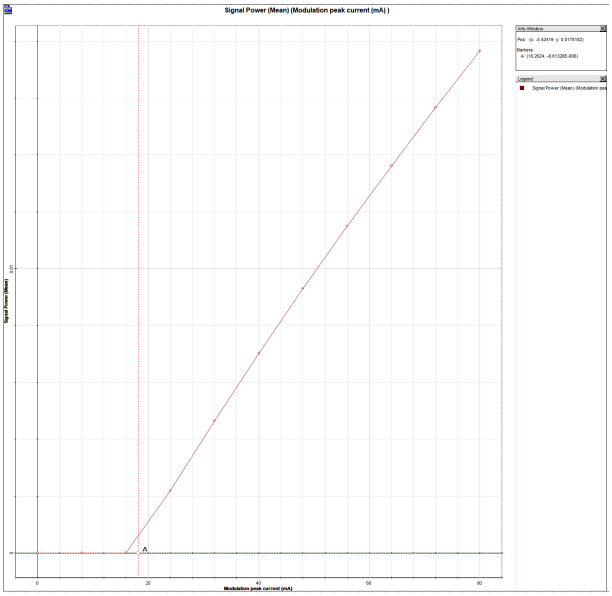

Fig. 3. L-I curve of parameter 2

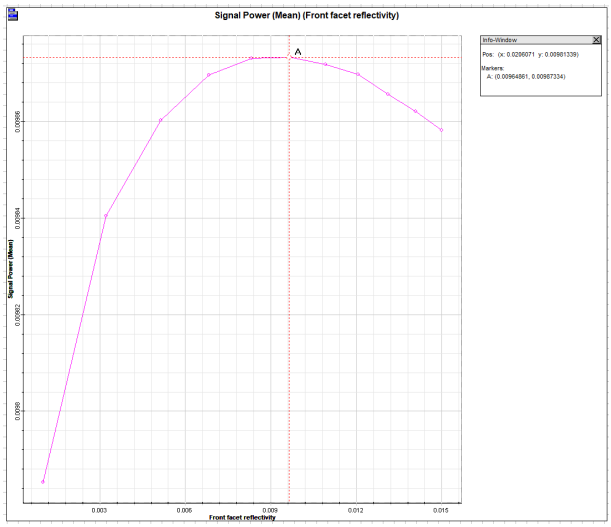

Fig. 4. Front Facet Reflectivity Optimization

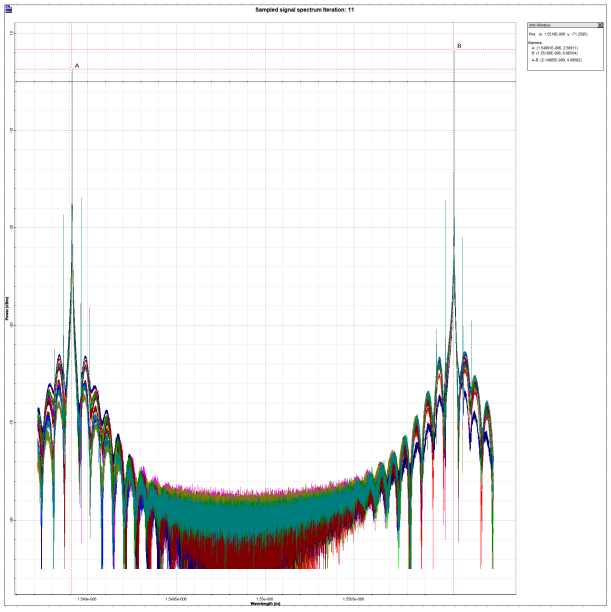

Fig. 5. Front Facet Reflectivity Optimization

optical feedback, while the modulation current controls the laser's output intensity and modulation characteristics. Careful consideration and optimization of facet reflectivity and modulation current are important for achieving reliable and high-performance operation of DFB lasers in various applications, including telecommunications and optical data transmission.

II. Multimode Optical Fiber Simulation

Multimode optical fiber is a type of fiber used in telecommunications and data networks to transmit multiple light paths simultaneously. It has a larger core diameter, allowing for more data transmission. However, it is limited to shorter distances due to modal dispersion. Multimode fiber is cost-effective and commonly used in LANs, data centers, and short-haul communications.

The critical angle is essential in multimode optical fiber as it determines the acceptance angle for light rays. It ensures efficient transmission by keeping the light signals within the core and minimizing signal loss. Optimizing the critical angle is crucial for maximizing the performance of multimode fiber.

Suppose the refractive index of fiber core is n_1, and for cladding is n_2, With snell's law:

$$n_1 sin(\theta_1) = n_2 sin(\theta_2) \tag{6}$$

When $\theta_2 = \pi/2$:

$$\theta_1 = arcsin(\frac{n_2}{n_1}) \tag{7}$$

For 850 wavelength:

$$V = \frac{2\pi a}{\lambda}\sqrt{n_1^2 - n_2^2} \approx 253.4 >> 1 \tag{8}$$

$$M = \frac{4}{\pi^2}M^2 \approx 26021.65 \tag{9}$$

Group velocity delay refers to the delay experienced by a group of photons or a light pulse as it propagates through a medium. It is important in optics and describes the speed at which the shape or envelope of a light pulse travels. It is relevant in optical communications to manage dispersion effects and ensure efficient transmission of information. Group delay of the sixth mode in the situation discussed:

$$\tau_g = \frac{L}{c}(N_{eff} - \lambda\frac{dN_{eff}}{d\lambda}) \tag{10}$$

$$= \frac{L}{c}(1.44751446007531 \tag{11}$$

$$-\lambda\frac{1.44751311049375 - 1.44751581124069}{0.2}) \tag{12}$$

$$\approx 4.866683us \tag{13}$$

The delay between different mode, for 0th and 9th mode as example:

$$\tau = \frac{L}{c/n_1 - c/n_2} \approx 0.076852s \tag{14}$$

The 0 mode has a larger refractive index, so that it moves slower than the 9th mode, thus the 9th mode will arrive earlier. The delay is shown above.

When light excites multiple modes in a multimode fiber, they propagate at different velocities due to their unique characteristics, causing the pulse to disperse and broaden as it travels. In the example with the first and tenth modes, the fundamental mode moves slower while the higher-order mode moves faster. This causes the pulse to spread out over time, reducing intensity and duration. Ultimately, this dispersion limits transmission capacity and degrades signal quality in long-distance multimode fiber systems.

The excited modes in a multimode fiber depend on the injected field. The amount of power coupled to specific mode can be calculated via an overlap integral. In special cases, like where the injected field is exactly the same as a specific fiber mode then all of the incident power will be coupled into that specific mode. In physical fibers, although one mode might be excited at the input of the fiber, power will spread to other modes through imperfections and bends.

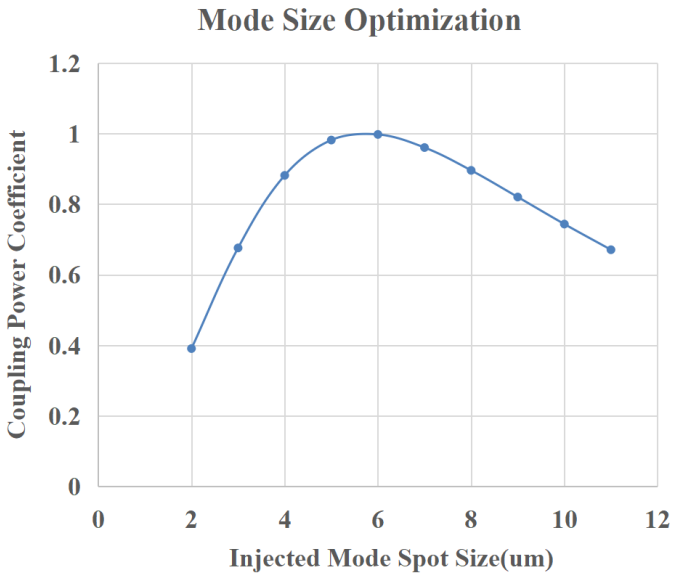

Fig. 6. Mode Size Optimization

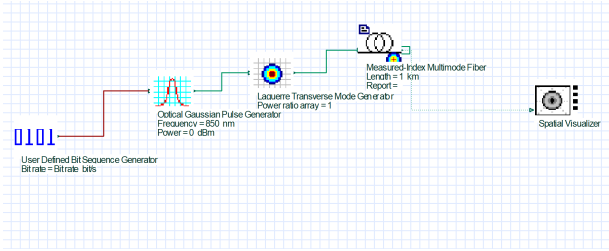

Fig. 7. Simulation Set up

Fig.6 shows the coupling power coefficient variation along with injected mode spot size varied from 2um to 11um under 1um resolution. It could be concluded that around 6um the maximum reaches.

III. Quadrature Amplitude Modulation Optical Transmitter

QAM (Quadrature Amplitude Modulation) is a widely used modulation technique in telecommunications and digital communication systems. It combines both amplitude and phase modulation to transmit digital data efficiently over a communication channel. By varying the amplitude and phase of a carrier signal, multiple bits of information can be encoded onto a single symbol, enabling higher data rates and improved spectral efficiency. QAM is particularly effective in applications such as wireless communication, digital television, and broadband internet, where it allows for the transmission of large amounts of data within limited bandwidth.

An MZI modulator is an optical device used in fiber optic communication systems to modulate light intensity or phase. It utilizes interference principles to control the output signal by adjusting the phase relationship between two arms. MZI modulators are widely used for signal modulation, wavelength conversion, and optical switching.

For MZI response:

$V_2 = -V_1$, the equation can be written as:

$$E_{out} = E_{in}[cos(\pi \frac{V_1}{V_\pi})] \tag{15}$$

$$V_1 = V(t) + V_{bias} \tag{16}$$

$$E_{out} = E_{in}[cos(\pi \frac{V(t) + V_{bias}}{V_\pi})] \tag{17}$$

For $V(t) \to 0$:

$$E_{out} = E_{in}[sin(\pi/2 - \pi \frac{V(t) + V_{bias}}{V_\pi})] \tag{18}$$

To obtain a linear respond, V_{bias} should be $V_\pi(1/2 + n)$.

When $V_{bias} = V_\pi/2$:

$$E_{out} = -E_{in} sin[\frac{\pi}{3} V(t)] \tag{19}$$

To achieve the highest sweep, $V(t)$ should equal to 1.5V, thus the gain of M-Pulsed Arrary should be 1.5. For -5V,-3V,-1V,1V,3V,5V, the gain should be 0.3,0.5 and 1.5.

Bit Sequence	I(t)	value	Q(t)	value	Bit Sequence	I(t)	value	Q(t)	value
000000	000	-7	000	-7	100000	100	1	000	-7
000001	000	-7	001	-5	100001	100	1	001	-5
000010	000	-7	010	-3	100010	100	1	010	-3
000011	000	-7	011	-1	100011	100	1	011	-1
000100	000	-7	100	1	100100	100	1	100	1
000101	000	-7	101	3	100101	100	1	101	3
000110	000	-7	110	5	100110	100	1	110	5
000111	000	-7	111	7	100111	100	1	111	7
001000	001	-5	000	-7	101000	101	3	000	-7
001001	001	-5	001	-5	101001	101	3	001	-5
001010	001	-5	010	-3	101010	101	3	010	-3
001011	001	-5	011	-1	101011	101	3	011	-1
001100	001	-5	100	1	101100	101	3	100	1
001101	001	-5	101	3	101101	101	3	101	3
001110	001	-5	110	5	101110	101	3	110	5
001111	001	-5	111	7	101111	101	3	111	7
010000	010	-3	000	-7	110000	110	5	000	-7
010001	010	-3	001	-5	110001	110	5	001	-5
010010	010	-3	010	-3	110010	110	5	010	-3
010011	010	-3	011	-1	110011	110	5	011	-1
010100	010	-3	100	1	110100	110	5	100	1
010101	010	-3	101	3	110101	110	5	101	3
010110	010	-3	110	5	110110	110	5	110	5
010111	010	-3	111	7	110111	110	5	111	7
011000	011	-1	000	-7	111000	111	7	000	-7
011001	011	-1	001	-5	111001	111	7	001	-5
011010	011	-1	010	-3	111010	111	7	010	-3
011011	011	-1	011	-1	111011	111	7	011	-1
011100	011	-1	100	1	111100	111	7	100	1
011101	011	-1	101	3	111101	111	7	101	3
011110	011	-1	110	5	111110	111	7	110	5
011111	011	-1	111	7	111111	111	7	111	7

Fig. 8. List of 64QAM

The highlighted point on the constellation figures are:

16QAM:4bits

(a) (-1,3) 0111

(b) (-3,-1) 0001

64QAM:6bits

(c) (1,5) 100110

(d) (7,-3) 111010

For 4 QAM:

The Layout Parameter Symbol rate should be set to 5 Gbaud. (Half of the bit rate), the maximum gain is 0.5.

For 64 QAM:

The Layout Parameter Symbol rate should be set to 3.333 Gbaud. (One-third of the bit rate), the maximum gain is 3/14.

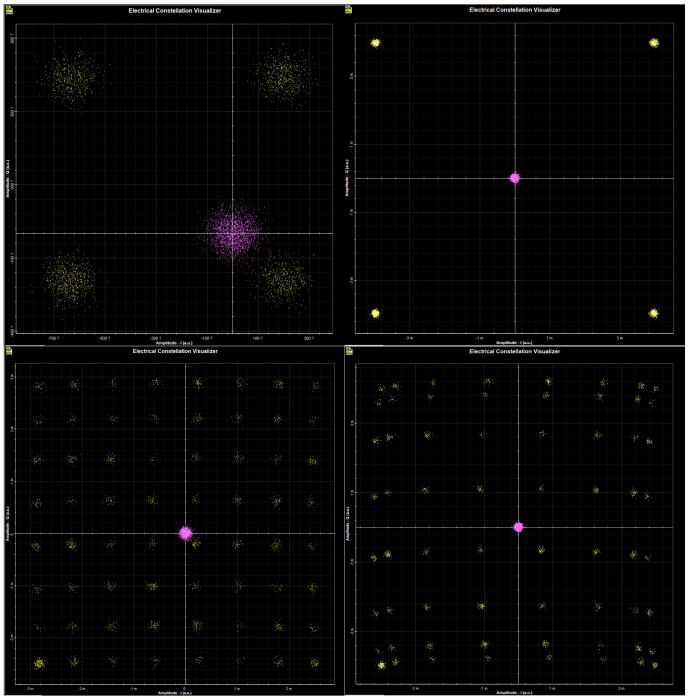

Fig. 9. left above: 4QAM with 0.1 electrical gain;right above:4QAM with max electrical gain;left below: 64QAM with 0.1 electrical gain;right below:64QAM with max electrical gain;

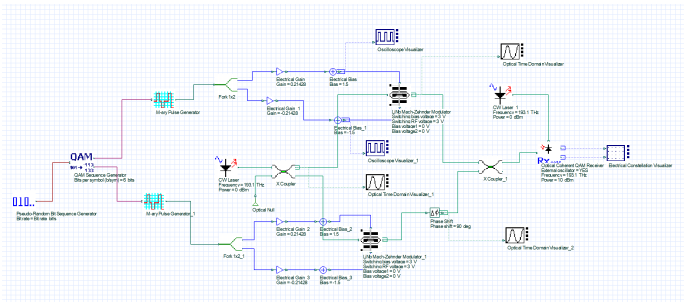

Fig. 10. Simulation Set up

It can be seen from the Fig.9 that, increasing electrical gain makes larger SNR, and the points are more densed and symmetrical than small gain. Under small gain, the influence of noise becomes significant and a entire bias of the points appears at the constellation.

When the gains of the arms in an MZI modulator are balanced but small, it can have a subtle impact on the QAM constellation diagram.

A balanced and small gain in the MZI arms means that the splitting ratio of the input signal into the two arms is relatively equal, and the modulation depth is not significantly affected. As a result, the amplitude and phase of the QAM signal remain relatively stable, and the constellation diagram is minimally distorted.

However, the small gain in the arms can lead to a decrease in the overall signal power. This reduction in power may affect the signal-to-noise ratio (SNR) of the QAM signal, potentially resulting in a higher bit error rate (BER) and reduced system performance. Additionally, the smaller gain might limit the

dynamic range of the modulator, impacting its ability to handle high-power or large-amplitude QAM signals.

To mitigate these effects, it is important to carefully design and optimize the gain balance in the MZI modulator, considering the desired signal power levels, system requirements, and performance targets. Proper power management techniques, including signal amplification before or after the modulator, can help to maintain an adequate SNR and optimize the QAM constellation diagram for reliable and efficient transmission.

IV. Conclusion

In conclusion, this thesis provided a comprehensive evaluation and analysis of the EE244 course project at Shanghaitech University. Utilizing the Optisystem software, the project involved simulation and extensive analysis of three critical aspects of the system: DFB laser parameter sweep, multi-mode fiber mode coupling, and the impact of gain on QAM modulation.

The exploration of DFB laser parameter sweep allowed for an intricate understanding of the influence of various laser parameters on system performance, highlighting the importance of correct laser parameter settings for effective communication.

The multi-mode fiber mode coupling simulation provided insight into the dynamic properties of fiber-optic transmission channels. It offered an in-depth understanding of the complexities and challenges of efficiently transmitting signals through multi-mode fibers and the implications on system performance.

Lastly, the study on the impact of gain on QAM modulation added valuable insights into the balance required between amplification and distortion/noise in digital communication systems. This part of the study underlined the need to carefully manage the gain for optimizing the quality of the received signal and minimizing the bit error rate.

Overall, the findings and results of this thesis have not only demonstrated an in-depth understanding of the complex processes in optical communication systems but also have potentially informed improved design and control strategies for these systems.

References

[1] Basil W. Hakki, Thomas L. Paoli; cw degradation at 300°K of GaAs double-heterostructure junction lasers. II. Electronic gain. Journal of Applied Physics 1 September 1973; 44 (9): 4113–4119. https://doi.org/10.1063/1.1662905

[2] Ghione, G. (2009). Semiconductor Devices for High-Speed Optoelectronics. Cambridge: Cambridge University Press. doi:10.1017/CBO9780511635595

[3] Vanzi, M. Optical Gain in Commercial Laser Diodes. Photonics 2021, 8, 542. https://doi.org/10.3390/photonics8120542

[4] M. Lerttamrab, S. L. Chuang, R. Q. Yang, C. J. Hill; Linewidth enhancement factor of a type-II interband-cascade laser. Journal of Applied Physics 15 September 2004; 96 (6): 3568–3570. https://doi.org/10.1063/1.1782269